



TITLE:

Gas Interchange between Bubble Phase and Continuous Phase in Gas-Solid Fluidised Bed at Coalescence

AUTHOR(S):

TOEI, Ryoza; MATSUNO, Ryuichi; NISHITANI, Keiichi

CITATION:

TOEI, Ryoza ...[et al]. Gas Interchange between Bubble Phase and Continuous Phase in Gas-Solid Fluidised Bed at Coalescence. Memoirs of the Faculty of Engineering, Kyoto University 1970, 32(2): 194-209

ISSUE DATE:

1970-09-10

URL:

<http://hdl.handle.net/2433/280817>

RIGHT:

Gas Interchange between Bubble Phase and Continuous Phase in Gas-Solid Fluidised Bed at Coalescence

By

Ryozo TOEI*, Ryuichi MATSUNO* and Keiichi NISHITANI*

(Received December 27, 1969)

By investigating the phenomena of coalescence of bubbles from the view point of gas interchange, the mechanism of interchange at coalescence in the case of two bubbles on the same vertical line was explained with the aid of Murray's method which gave the gas stream function.

CO₂ gas bubbles were blown into a two dimensional air-fluidised bed at the point of minimum fluidisation through a single nozzle. The concentration of the bubble and of the continuous phase was measured and the gas interchange coefficient was obtained. From it, the amount of gas that flowed out from the cloud was obtained and it coincided fairly well with that obtained from the gas stream line.

Although the experimental system was a special case where bubbles were formed only from a single nozzle, the method for obtaining the gas interchange coefficient, that includes the effect of coalescence, was explained if the distribution of the frequency and the rising velocity of the bubble were known.

§ 1. Introduction

Gas interchange between the bubble phase and the continuous phase is very important in the operation of a gas-solid fluidised system. The authors have already studied this subject, between a single bubble and the continuous phase in a two dimensional fluidised bed¹⁰⁾.

However, since the coalescence of bubbles occurs frequently, this effect on the gas interchange should also be considered. Muchi et al.²⁾ investigated the behaviour of gas around bubbles at coalescence and pointed out the important effects of coalescence.

Furthermore, the authors have also studied the mechanism of coalescence of two bubbles, based on the motion of each.⁸⁾

In this work, gas interchange between bubbles and continuous phase brought

* Department of Chemical Engineering

about by coalescence was investigated.

① The gas stream line around two bubbles when these were on the same vertical axis and coalesced in a two dimensional fluidised bed was obtained by Murray's method³⁾, and the amount of gas which flowed out from the cloud to the continuous phase during this process was calculated.

② Motion of the gas expelled from the bubble during coalescence was observed by blowing two NO₂ gas bubbles into a two dimensional air fluidised bed at the point of minimum fluidisation with a short time interval between them and was compared with the calculated results from ①.

③ CO₂ gas bubbles were blown continuously through a single nozzle into an air-fluidised bed held at the point of minimum fluidisation. The concentration of CO₂ gas in the bubble and in the continuous phase was measured at various positions in the bed. Thus, the gas interchange coefficient for the case of coalescence was obtained.

A model was proposed in which this coefficient was assumed to be the sum of the gas interchange coefficient of an isolated rising bubble and that at coalescence. The amount of gas that flowed out from the clouds during one coalescence was obtained based on the experimental values of the gas interchange coefficients.

This was compared with that obtained from the calculation of ①.

§ 2. Gas flow in the case of two bubbles rising on the same vertical axis in the two dimensional fluidised bed, and the calculation of the amount of gas that flows out from the clouds during a coalescence.

Using the complex potential for the particles when two bubbles of the same radius a are rising on the same vertical axis with a distance c between their centres in the two dimensional case the complex potential of the gas is obtained by Murray's method³⁾.

The non dimensional complex plane z is considered. The origin of the coordinate is at the centre of the upper bubble. The real axis is in the direction of the bubble movement and the imaginary axis is in the perpendicular direction. By assuming that the motion of the particle around the bubbles is that of an ideal fluid around two cylinders, the non dimensional complex potential of the particle flow relative to the upper bubble is obtained as follows³⁾,

$$W_p(z) = -\alpha z - \alpha \left[\sum_{n=0}^{\infty} \frac{\mu_n^*}{z - z_n^*} + \frac{\alpha'}{\alpha} \sum_{n=0}^{\infty} \frac{\mu_n^*}{z - z_n^*} \right] \quad (1)$$

Where z and $W_p(z)$ are non dimensional quantities with respect to the radius of

bubble a and the product of the interstitial gas velocity U_0 and a respectively. Further,

$$\begin{aligned} \alpha &= U/U_0, & \alpha' &= V/U_0, & \mu_n^* &= \mu_n/a^2, & z_n^* &= -f_n/a, \\ z_n'^* &= -(c-f_n)/a, & f_0 &= 0, & \mu_0 &= a^2 \\ \text{for odd } n, & f_n &= c - \frac{a^2}{c-f_{n-1}}, & \mu_n &= -\mu_{n-1} \frac{a^2}{(c-f_{n-1})^2} \\ \text{for even } n, & f_n &= \frac{a^2}{f_{n-1}}, & \mu_n &= -\mu_{n-1} \frac{a^2}{f_{n-1}^2}. \end{aligned}$$

In Murray's method⁹⁾, the convective term of the equation of motion is approximated by Oseen's linearization⁴⁾. In addition to this, the following assumption is made:—

Although coalescence is an unsteady phenomenon, it is assumed that the system is instantly in a steady state. With these two assumptions, the next equation is obtained,

$$W_f(z) = z + W_p(z) - c'F\alpha \left[\alpha + \frac{dW_p(z)}{dz} \right] \quad (2)$$

By substituting Eq. (1) into Eq. (2), the following equation is obtained.

$$\begin{aligned} W_f(z) &= -(\alpha-1)z - \alpha \left[\sum_{n=0}^{\infty} \frac{\mu_n^*}{z-z_n^*} + \frac{\alpha'}{\alpha} \sum_{n=0}^{\infty} \frac{\mu_n^*}{z-z_n'^*} \right. \\ &\quad \left. - c'F\alpha^2 \left[\sum_{n=0}^{\infty} \frac{\mu_n^*}{(z-z_n^*)^2} + \frac{\alpha'}{\alpha} \sum_{n=0}^{\infty} \frac{\mu_n^*}{(z-z_n'^*)^2} \right] \right] \quad (3) \end{aligned}$$

In Eq. (3), $c'F\alpha^2$ was taken as $1/4$. This was the same value obtained by Murray for a single bubble.

Although α and α' should be chosen so as to make the pressures near the top surfaces of the upper and lower bubbles constant, the experimental result of previous works^{8,9)} on coalescence in the same vertical line (Fig. 5 of reference 8) and Fig. 1 of 9) was used.

$W_f(z)$ is written as

$$W_f(z) = \phi_f + i\psi_f \quad (4)$$

From Eqs. (3) and (4), the stream function of the gas flow and the velocity distribution of the gas around the bubbles are obtained. From this velocity, the movement of gas elements whose initial positions at the beginning of the process of coalescence are at the surface of the clouds of the upper and lower bubbles can be calculated numerically (by computer) for the case of one coalescence.

Results for the cloud of the upper bubble are shown in Fig. 1. The critical non dimensional distance c^* between the centres of the bubbles within which coales-

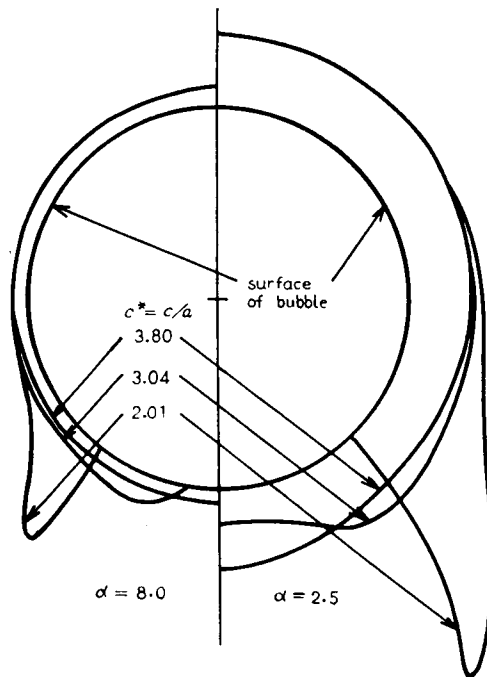


Fig. 1. Drift line of cloud surface of upper bubble during a process of coalescence.

cence is possible is $4.0^{9)}$. However, if the calculation is started from $c^*=4.0$, the bubbles never coalesce since the rising velocities of the upper and lower bubbles are the same at $c^*=4.0$. So, the calculation was started taking initial distance as $c^*=3.8$. It is clearly shown in Fig.1 that the gas elements which were at the surface of the cloud at $c^*=3.8$ flow out from the lower part of the cloud with a decrease of the distance between the centres of the bubbles. Furthermore, the greater the amount of gas that flows out from the cloud is, the larger the particle size, i.e., the smaller the value of α . That is, the effect of coalescence is considerably greater the larger the particle size.

Although gas flows out from the cloud of the lower bubble also, its amount is not very large. The rising velocity of the lower bubble changes continuously during $c^*=3.8$ to 2.28 and is 2.7 times larger than that of the upper bubble during $c^*=2.28$ to 2.0 as shown in the previous paper^{8,9)}. Although the time interval during $c^*=2.28$ to 2.0 is short, the rate of outflow of gas is considerable.

During the period from $c^*=2.0$ to 0.0, that is the period after the lower bubble overtakes the bottom of the wake of upper one, Eq. (3) has no significance. In this paper the calculation for this period was carried out by the expedient method to be

referred to later. However, since it is an approximate method, the gas flow after the lower bubble overtakes the upper one should be further investigated.

Two visible brown NO_2 gas bubbles were blown into a two dimensional air fluidised bed at the point of minimum fluidisation during a short time interval and were photographed with a 16mm cine camera. The apparatus was basically the same as that used in the previous work¹⁰.

A sketch from the film is shown in Fig. 2. Fig. 2A refers to the coalescence of bubbles on a common vertical axis and B refers to the case when they are not on the same vertical line. The particles used are 42~48 μ glass beads in both cases and α is small ($\alpha \approx 2$).

Qualitatively, the behaviour of NO_2 gas around the upper bubble shown in Fig. 2A coincides fairly well with the calculated behaviour of the gas shown in Fig. 1. The outflow of gas decreased with increase in α as predicted although the experimental result for larger α is not shown in Fig. 2.

The following patterns of behaviour of NO_2 gas are shown in Fig. 2A.:

The gas within the cloud of the upper bubble flows out down-stream and the cloud of the lower bubble is sucked into the upper one as shown in Fig. 2A (i) and (ii). During this process, the dense phase gas between the upper and lower bubbles flows into the upper one. With lapse of time, the gas that flowed out from the

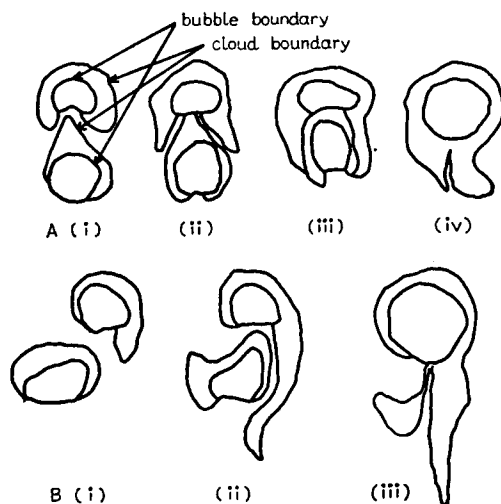


Fig. 2. Sketch of the behaviour of NO_2 gas around the bubbles during a process of coalescence (42~48 μ glass beads).

A. In the case of coalescence of two bubbles standing on the vertical line.

B. In the case of coalescence of two bubbles not standing on the vertical line.

upper cloud surrounds the NO₂ of the lower bubble as shown in (iii), but the boundary of NO₂ of both upper and lower bubbles remains distinct.

When the two bubbles have become one roughly stable single bubble after coalescence, NO₂ gas that flowed out down-stream is left behind.

The amount of gas lost from the clouds of upper and lower bubble after one coalescence, should mean that which was inside the clouds of both at the beginning and is left behind the cloud of the stable single bubble formed by coalescence. However, since Eq. (3) has no significance during $c^*=2.0$ to 0.0 as mentioned above, calculations like those shown in Fig. 1 cannot be carried out. So the amount of the gas $K[\text{cm}^2]$ that flowed out during one coalescence was calculated by the following expedient method.

The amount of gas that flowed out from the cloud of the upper bubble at $c^*=3.8$ to 2.0, that is, the area surrounded by the cloud surface at $c^*=3.8$ and its drift line at various c^* is calculated by graphical integration on Fig. 1 and is multiplied by ε_{mf} . The rate of outflow is calculated by differentiating the above quantity with respect to time.

An example of this is shown in Fig. 3 by the solid curve. The abscissa is the dimensionless time t^* and the ordinate is the dimensionless rate of outflow Q . Q is obtained by differentiating the amount of outflow with respect to dimensionless time t^* and being divided by d_b^2 .

The rate of outflow during $c^*=2.0$ to 0.0 is assumed approximately as that near $c^*=2.0$, since Eq. (3) cannot be used.

It is shown in Fig. 3 by the dotted line. The amount of gas which flowed out

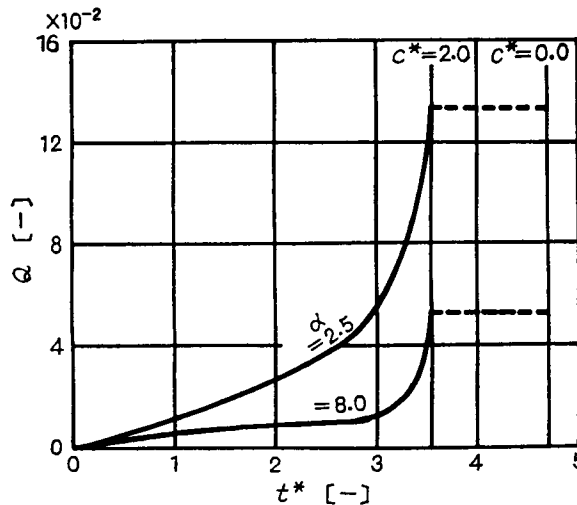


Fig. 3. Flowing out rate of gas from the cloud of upper bubble.

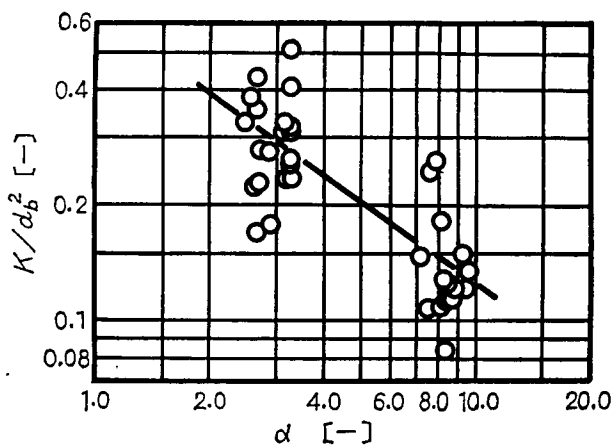


Fig. 4. Amount of gas flowing out from the clouds by one coalescence. Solid line shows the calculated value from the stream line.

from the cloud of the upper bubble is obtained by multiplying the area under the solid curve and dotted line by d_b^2 .

The same process is repeated for the lower bubble. Then, the total amount of outflow, K is the sum of these.

Since Eq. (3) is a dimensionless equation with respect to a and U_0 , and the drift line of the cloud surface calculated from it is similar to Fig. 1 with the same α even if the bubble diameter changes, K is proportional to d_b^2 and then K/d_b^2 is a function of α only. The calculated result is shown in Fig. 4 by a solid line. The amount which flowed out from the cloud of the lower bubble is about 20~30% of K .

In this way the amount of the gas flowing out from the cloud is calculated and an equal amount flows into the clouds from the continuous phase.

For the sake of simplicity, the calculation was only carried out for the case of the same bubble size as in Fig. 4. However, the coalescence of various bubble size ratios takes place in actual fluidised bed.

Fig. 2 B shows, sketched from the film, the behaviour of NO_2 gas at coalescence of bubbles not lying on the same vertical axis.

It differs very much from that of coalescence on the same vertical axis. Although the calculation for coalescence not on the same vertical axis is difficult, the investigation for this case is necessary since in reality it takes place with a relatively high frequency.

§ 3. Experiments with CO_2 gas and discussion.

CO_2 gas bubbles were blown into a two dimensional air-fluidised bed at the

point of minimum fluidisation through a single nozzle installed at the centre of the bottom. Then, the distribution of the concentration of the bubbles, in the vertical direction, and of the time average concentrations in the bed were measured and the gas interchange coefficient was obtained.

3.1 Experimental apparatus, method and conditions

The fluidised bed apparatus used was almost the same as that used in previous work¹⁰⁾ and the width, thickness and height were 40 cm, 1.5cm and 120cm respectively. The sampling device for the gas in the bubble was the same as previously¹⁰⁾. Fig. 5 shows a schematic diagram of the sampling device for continuous phase gas and it consists of the installation device *A* and the pipette *B* (volume \approx 100 cc). By opening both cocks of the pipette by a suitable amount, the gas in the bed is discharged spontaneously at a suitable rate due to the pressure difference between the bed and outside.

The maximum discharge rate of gas that did not effect the fluidising behaviour

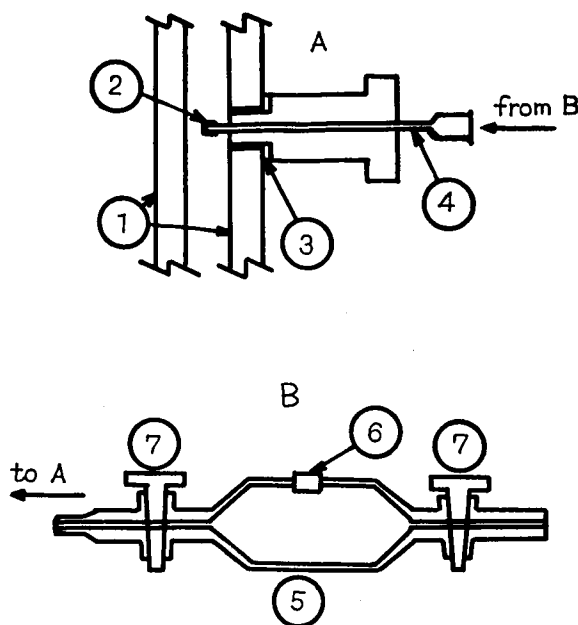


Fig. 5. Schematic diagram of sampling section of continuous phase.

- ① Wall of two dimensional fluidised bed
- ② 200# sieve
- ③ Packing
- ④ Needle of injector 1 ϕ I. D.
- ⑤ Sampling pipette ca. 100 cc
- ⑥ Rubber stopper
- ⑦ Two ways cock

Table 1. Experimental condition

Particle	u_{mf} [cm/sec]	ε_{mf} [-]	Run.	Temp. [°C]	CO ₂ rate [cc/sec]	Air rate [cc/sec]
42~48# glass beads	8.20	0.400	1	19.2	554	548
			2	20.0	383	545
			3	21.0	267	545
80~100# glass beads	2.47	0.408	4	21.0	274	151
			5	17.0	175	160

was about 50 cc/min. The gas in the pipette was sampled from the rubber stopper by the gas sampler of gas chromatography while discharging the gas and the concentration was analysed by gas chromatography. The sampling was continued until the concentration in the pipette became constant. The time required for obtaining constant concentration was on the average five minutes.

The whole of the fluidised bed was photographed using a 16mm cine camera and the frequency distribution and the velocity of bubble rise were measured.

Since sampling of the gas in the bubble and in the bed and photography with the 16mm cine camera could not be carried out simultaneously, they were done separately.

Experimental conditions are shown in Table 1.

The particles used were 42~48# and 80~100# glass beads.

3.2 Experimental results and discussion

3.2.1 Calculation method for the gas interchange coefficient k_{gT} based on the surface of the bubble.

It is assumed that the voidage fraction of cloud is ε_{mf} and the concentration in the cloud is the same as that in the bubble.

Taking the mass balance for the cloud of one bubble, for a short time interval with respect to the tracer gas, Eq. (5) is obtained.

$$V_c \frac{dc_b}{dt} + k_{gT} \frac{4}{d_b} V_b (c_b - c_f) = 0, \quad (5)$$

where

$$V_c = V_b [1 + \varepsilon_{mf} (V_c' / V_b - 1)]. \quad (6)$$

V_c' / V_b is the ratio of the cloud volume including the particle volume to the bubble volume and is a function of α . V_c is the volume of the cloud excluding the particle volume. The relation between the rising distance of the bubble and the time is

$$dx = U dt. \quad (7)$$

From the above equation, the gas interchange coefficient k_{gT} based on the bubble surface can be determined experimentally.

In the next section, a description is given of the various values which are necessary in order to calculate k_{gT} .

3.2.2. Frequency, rising velocity and diameter of bubble.

The frequency n and the rising velocity of the bubble were measured from the 16mm cine film. The relation between the frequency of the bubble and height of bed could be almost represented by a single curve approximately independent of the flow rate, as could be done with the previously reported results⁹. The effect of particle size was also small. The results are shown in Table 2 (average values). The measured rising velocities are also shown in Table 2.

The bubble diameter was obtained as follows. At first, it was assumed that the gas flow rate blown into the bed through nozzle became the cloud flow rate.

On the other hand, the relation between α and V_c'/V_b was obtained from NO_2 gas experiments for a single bubble. The results coincided well with the results

Table 2 Partial list of experimental results

Run	x [cm]	n [1/sec]	U [cm/sec]	v_c/v_b [—]	d_b [cm]	c_b [—]	c_f [—]	k_{gT} [cm/sec]	k_{gT}/k_{gt} [—]	α [—]	K [cm ²]	K/d_b^2 [—]
1	10	5.05	59.0	1.176	8.95	0.906	0.320	2.318	2.43	2.88	14.31	0.179
	30	2.52	66.0	1.144	12.79	0.780	0.370	2.473	2.38	3.22	41.15	0.252
	50	1.92	68.0	1.140	14.67	0.720	0.404	1.979	1.80	3.32	50.47	0.235
	70	1.67	68.0	1.140	15.50	0.688	0.428	1.548	1.37	3.32	73.47	0.306
2	10	5.05	54.0	1.208	7.33	0.880	0.329	2.083	2.40	2.63	11.86	0.221
	30	2.52	63.0	1.160	10.52	0.754	0.376	2.339	2.42	3.07	33.92	0.306
	50	1.92	66.0	1.148	12.20	0.680	0.404	2.009	1.97	3.27	46.22	0.311
	70	1.67	67.0	1.148	12.98	0.641	0.421	1.634	1.56	3.27	85.90	0.509
3	10	5.05	51.0	1.224	6.09	0.847	0.331	3.247	2.71	2.49	12.22	0.330
	30	2.52	54.0	1.204	8.66	0.688	0.357	2.126	2.34	2.64	28.91	0.434
	50	1.92	55.0	1.196	10.00	0.619	0.370	1.519	1.60	2.68	27.74	0.227
	70	1.67	55.0	1.196	10.53	0.581	0.375	1.093	1.13	2.68	18.50	0.167
4	10	4.93	49.0	1.102	6.72	0.918	0.480	1.450	1.646	8.10	4.98	0.110
	30	2.47	52.0	1.102	8.84	0.826	0.546	1.311	1.402	8.65	8.71	0.112
	50	1.71	56.0	1.102	11.18	0.788	0.595	1.372	1.372	9.26	16.60	0.132
	70	1.45	57.0	1.102	12.25	0.768	0.621	1.220	1.197	9.42	20.0	0.133
5	10	4.93	43.5	1.098	5.38	0.905	0.555	1.374	1.618	7.19	4.15	0.144
	30	2.47	47.0	1.098	7.08	0.805	0.606	1.470	1.686	7.76	12.3	0.245
	50	1.71	49.0	1.098	8.95	0.760	0.630	1.297	1.380	8.10	14.5	0.181
	70	1.45	51.0	1.098	9.80	0.742	0.639	1.051	1.095	8.43	8.11	0.083

of Rowe et al.⁹⁾ and Murray's equation⁹⁾. Since the frequency and the rising velocity of the bubble had been obtained at various heights of the bed, V_c of Eq. (6) was obtained by dividing the flow rate at nozzle by the frequency. V_c'/V_b was obtained from the rising velocity and finally, V_b and d_b were obtained from Eq. (6). V_c/V_b and d_b are shown in Table 2.

The above assumption that the flow rate at the nozzle became the cloud flow rate differed from the two phase theory¹²⁾. However, since the following factors were known, the above assumption was made.

① It was shown in a previous paper⁷⁾ that the two phase theory did not hold when the particle size was large, that is, the flow rate in the continuous phase is greater than the minimum fluidisation flow rate. ② For a given volume of gas blown into the bed as a single bubble, the bubble volume is smaller the larger the particle size. ③ It was known from the NO_2 gas experiments that a cloud was formed at the instant of bubble injection. ④ Rowe et al.⁹⁾ stated that the gas flow rate above minimum fluidisation flow rate flowed as clouds.

3.2.3. Concentration of bubble and continuous phase.

The CO_2 gas concentration of the bubble in the vertical direction is shown in Fig.6 and in Table 2.

Examples of the time average concentration in the bed are shown in Fig. 7.

The bed is divided into vertical strips.

The ratio of the inter phase area between the bubble and the continuous phase, included in one division, to the total inter phase area at a given bed height changes from division to division in this experiment and so differs from the normal fluidised bed.

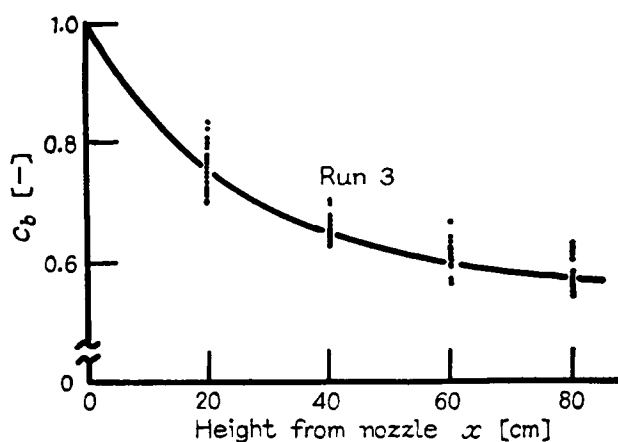


Fig. 6. An example of distribution of CO_2 gas concentration of bubble in the vertical line.

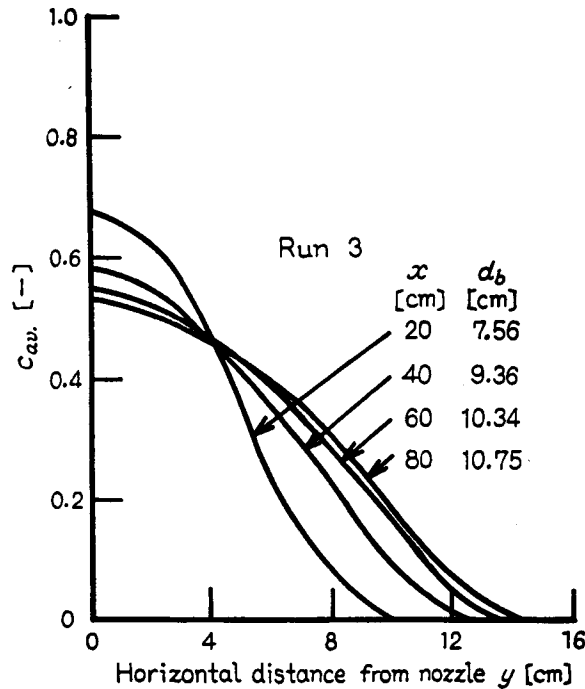


Fig. 7. Local time average CO₂ gas concentration in the bed.

The ratio is small on the vertical axis above the nozzle and increases with the distance away from the central axis.

It has a maximum value at y equal to the cloud radius and is zero at y larger than this. There is a resistance of the gas mixing in a horizontal direction in these experiments.

For the above reasons, the time average concentration in the bed shows the distribution in the horizontal direction as in Fig. 7.

Then c_f in Eq. (5) should be taken as the value which is obtained by averaging the concentration of the continuous phase at an arbitrary position in the y direction by weighing the ratio of the inter phase area between the bubble and the continuous phases which passes through that division to the total inter phase area.

Since the time average concentration c_{av} in the bed means the time average concentration of the bubble and the continuous phases, the concentration in the continuous phase can be obtained from c_{av} as follows.

Since the frequency, rising velocity and cloud diameter of bubble are known, the ratio of the average time when the sampling position is covered by the bubble phase to that of the continuous phase is calculated.

Then the concentration of continuous phase is calculated from it by using the

known concentration in the bubble phase and the time average concentration in the bed.

From this concentration of the continuous phase, c_f is obtained by an averaging method. But the above method has the following two defects.

① As the pressure difference between the bed and outside when the sampling point is covered by the bubble phase differs from that when it is covered by the continuous phase, the correct time average concentration can not be obtained at the point where bubble phase passes through. ② When the bubbles coalesce, the gas which flows out from the top of the lower cloud into continuous phase reenters into the upper bubble as shown in Fig. 2A. Although such gas should be considered as the gas of the bubble phase, it is calculated as the gas of the continuous phase in the above mentioned calculating method.

Instead of the above method, the time average concentration at the radius of the cloud in a horizontal direction (which is now equal to the concentration of the continuous phase) is taken approximately as the concentration of continuous phase c_f under the assumption that the gas of the continuous phase is well mixed where

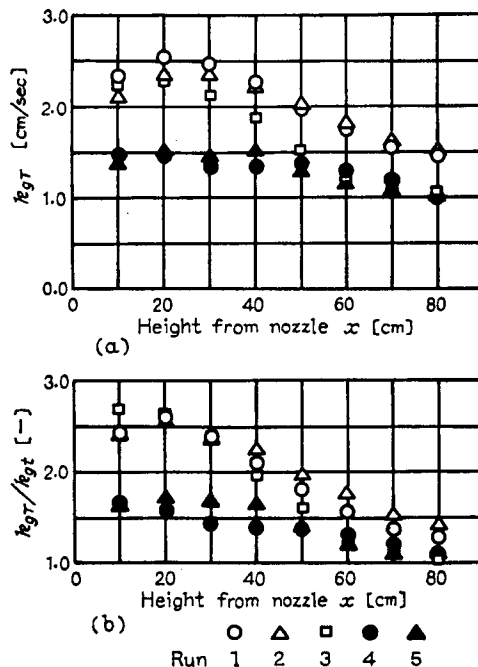


Fig. 8. (a) Gas interchange coefficient based on the surface of bubble.

(b) Ratio of gas interchange coefficient involving the coalescence to that for single bubble.

the bubbles pass through. It is shown in Table 2.

3.2.4. Gas interchange coefficient based on the surface of the bubble.

By substituting the above mentioned values into Eq. (5), (6) and (7), k_{gT} was obtained. The results are shown in Table 2 and Fig. 8 (a), and the ratio of k_{gT} to the gas interchange coefficient for the single bubble k_{gt} that was obtained from the model of previous paper¹⁰⁾ at the same condition for which k_{gT} was obtained is shown also in Table 2 and Fig. 8 (b).

It is known from these results that k_{gT} is large at the lower part of the bed where the frequency of coalescence is very high, and is small at the higher part of the bed where it is less. Further, as shown in Fig. 8 (b), k_{gT} becomes close to the gas interchange coefficient for a single bubble in the upper part of the bed.

At the lower part of the bed the interchange coefficient for the larger particle size, that is, smaller α , is large. It means that the effect of the coalescence is greater the larger the particle size as mentioned in § 2. The effect of the gas flow rate at the nozzle is small.

3.2.5. The amount of gas that flows out from (or into) the cloud.

If a model is assumed that gas interchange due to the single bubble motion and interchange due to coalescence occur in parallel, and k_{gT} obtained in the experiment is the sum of the two interchange coefficients, the amount of gas K that flows out from (or into) the cloud is obtained by the following equations.

$$k_{gT} = k_{gt} + \frac{K}{\pi d_b} \left(-\frac{dn}{ndx} \right) U \quad (8)$$

The first term of the right hand side is the gas interchange coefficient for the single bubble obtained from the model of the previous paper¹⁰⁾.

Since k_{gT} was obtained from the mass balance for the cloud in present work, k_{gt} which was not multiplied by the volume correction factor¹⁰⁾ is used. $(-dn/ndx)$ in the second term is the number of coalescences per bubble during a rise of 1 cm..

K was obtained by substituting experimental values of k_{gT} and calculating k_{gt} in Eq. (8) and is plotted in Fig. 4. Although the experimental points scatter very much, they broadly follow the values obtained in § 2.

It is known from Fig. 4 that the effect of the coalescence is very much more for small α and is smaller for large α , that is, smaller particle size or smaller particle density. In a catalytic reaction, u_{mf} is very small because of the small particle size and density. So, in general α is very large and the effect of coalescence is very small except in the lower part of the bed.

From the above results, the gas interchange coefficient that includes the effect of the coalescence is obtained if the distribution of the frequency and the rising

velocity of the bubble are known.

§ 4. Summary and Conclusion

① By investigating the phenomena of coalescence of bubbles from the view point of gas interchange, the mechanism of interchange at coalescence for the case of two bubbles on the same vertical line was explained with the aid of Murray's method which gave the gas stream function.

② CO₂ gas bubbles were blown into a two dimensional air-fluidised bed at the point of minimum fluidisation through a single nozzle. The concentration of the bubble and of the continuous phase were measured and the gas interchange coefficient was obtained. From it, the amount of the gas that flowed out from the cloud was obtained and it coincided fairly well with that obtained from the gas stream line.

③ Although the experimental system was the special case where bubbles were formed only from a single nozzle, the method for obtaining the gas interchange coefficient, that includes the effect of coalescence, was explained if the distribution of the frequency and the rising velocity of the bubble were known.

Fortunately, the curves of the frequency distribution of the bubble along the bed height obtained by many investigators are in good agreement. It can be expected that the gas interchange coefficient including the effect of coalescence can be obtained from the frequency curve together with an understanding of the mechanism of coalescence. So, here after, the investigation of gas interchange at coalescence for the case where bubbles do not lie all in the same vertical axis and the present work's extension to three dimensional bed should be carried out.

Nomenclature

a	=radius of bubble	[cm]
c	=distance between the centers of two bubbles	[cm]
c^*	= c/a , dimensionless distance between the centers of two bubbles	[—]
c_{av}	=local time average concentration in the bed	[—]
c_b, c_f	=concentration of bubble phase and continuous phase	[—]
c'	=the constant introduced by Murray ³⁾	[—]
d_b	=diameter of bubble	[cm]
F	= U_0^2/ga , Froude number	[—]
g	=acceleration of gravity	[cm/sec ²]
G_c	=flow rate of CO ₂ gas at nozzle	[cm ³ /sec]
i	=unit complex number	[—]

k_{gT}	=gas interchange coefficient based on the surface of bubble	[cm/sec]
k_{gt}	=gas interchange coefficient for a single bubble	[cm/sec]
K	=amount of gas which flowed out from the clouds during a coalescence	[cm ²]
n	=frequency of bubble	[numbers/sec]
Q	=non-dimensional flowing out rate of gas from the cloud	[—]
t	=time	[sec]
t^*	=non-dimensional time, $(U \cdot t)/a$	[—]
u_{mf}	=minimum fluidising velocity	[cm/sec]
U	=rising velocity of upper bubble or bubble	[cm/sec]
U_0	= u_{mf}/ϵ_{mf} interstitial gas velocity	[cm/sec]
V	=rising velocity of lower bubble	[cm/sec]
v_b	=volume of bubble	[cm ³]
v_c	=volume of cloud excluded particle volume	[cm ³]
v_c'	=volume of cloud included particle volume	[cm ³]
$w_f(z)$	=non-dimensional complex potential of gas	[—]
$w_p(z)$	=non-dimensional complex potential of particle	[—]
x	=vertical height from nozzle	[cm]
y	=horizontal distance from nozzle	[cm]
z	=non-dimensional complex coordinate	[—]
α	= U/U_0	[—]
α'	= V/U_0	[—]
ϵ_{mf}	=void fraction at minimum fluidising state	[—]
ϕ_f	=non-dimensional velocity potential of gas	[—]
ψ_f	=non-dimensional stream function of gas	[—]

Literature cited

- 1) Milne-Thomson, L. M.: "Theoretical Hydrodynamics" 4th edition Lond., Macmillan (1960).
- 2) Muchi, I., Mori, S. and Shichi, R.: *Kagaku Kogaku*, **32**, 343 (1968).
- 3) Murray, J. D.: *J. Fluid. Mech.*, **22**, 57 (1956).
- 4) Lewis, J. A. and Carrier, F. G.: *Quart. Appl. Math.*, **7**, 228 (1949).
- 5) Rowe, P. N., Partridge, B. A. and Lyall, E.: *Chem. Eng. Sci.*, **19**, 973 (1964).
- 6) Rowe, P. N. and Partridge, B. A.: *Trans. Instn. Chem. Engrs.*, **43**, 157 (1966).
- 7) Toei, R., Matsuno, R. and Fujiki, I.: *Kagaku Kogaku (Chem. Eng., Japan)*, **31**, 398 (1967).
- 8) Toei, R., Matsuno, R. and Sumitani, T.: *Kagaku Kogaku (Chem. Eng., Japan)*, **31**, 861 (1967); "Proc. of International Sympo. on Fluidisation" p271 (1967) Netherlands univ. press.
- 9) Toei, R., Matsuno, R. and Mori, M.: *Kagaku Kogaku*, **32**, 104 (1968).
- 10) Toei, R., Matsuno, R., Miyagawa, H., Nishitani, K. and Komagawa, Y.: *Kagaku Kogaku*, **32**, 565 (1968); *Int. Chem. Eng.* **21**, 358 (1969); *Mem. of Fac. Eng. Kyoto Univ.* **30**, part 4 525 (1968).
- 11) Toomey, R. D. and Johnstone, H. F.: *Chem. Eng. Progr.*, **48**, 220 (1952).